Structural Engineering and Mechanics, Vol. 27, No. 3 (2007) 365-391
DOI: http://dx.doi.org/10.12989/sem.2007.27.3.365

Vibration and stability of composite cylindrical shells containing a FG layer subjected to various loads

A.H. Sofiyev†

Department of Civil Engineering of Suleyman Demirel University, Isparta, Turkey

(Received February 17, 2006, Accepted March 10, 2007)

Abstract. The vibration and stability analysis is investigated for composite cylindrical shells that composed of ceramic, FGM, and metal layers subjected to various loads. Material properties of FG layer are varied continuously in thickness direction according to a simple power distribution in terms of the ceramic and metal volume fractions. The modified Donnell type stability and compatibility equations are obtained. Applying Galerkin's method analytic solutions are obtained for the critical parameters. The detailed parametric studies are carried out to study the influences of thickness variations of the FG layer, radius-to-thickness ratio, lengths-to-radius ratio, material composition and material profile index on the critical parameters of three-layered cylindrical shells. Comparing results with those in the literature validates the present analysis.

Keywords: FG layer; vibration and stability; composite cylindrical shell; buckling loads; frequency parameter.

1. Introduction

Functionally graded materials (FGM) are characterized by a gradual change in properties within the specimen as a function of the position coordinates. The property gradient in the material is typically caused by a position-dependent chemical composition, micro structure or atomic order. There are several studies about the processing of FGM, and an overview of the different manufacturing methods can be found in Kieback *et al.* (2003). There are two major groups of manufacturing methods. In the first class, known as constructive processes, the gradients are produced by selectively stacking two or more different materials. In the second class, known as transport-based processes, transport phenomena is used to create compositional and micro structural gradients during the production of a component (Koizumi 1993, Mortensen and Suresh 1995). These manufacturing processes include: centrifugal casting, electrohoretic deposition, spark plasma sintering, and directed vapor deposition, among others (Groves and Wadley 1997, Biesheuvel and Verweij 2000, Shen and Nygren 2002, Put *et al.* 2003).

A formulation of the stability problem for functionally graded hybrid composite plates, where a micro mechanical model was employed to solve the buckling problem for rectangular plates subjected to uniaxial compression presented by Birman (1995). Feldman and Aboudi (1997) studied elastic bifurcation buckling of FG plates under in-plane compressive loading. In this work they

† Professor, Dr. E-mail: asofiyev@mmf.sdu.edu.tr

assumed that grades of material properties throughout the structure are produced by a spatial distribution of the local reinforcement volume fraction. Reddy and Chin (1998) studied thermo-mechanical analysis of functionally graded cylinders and plates. Loy *et al.* (1999) presented a free vibration analysis of simply supported cylindrical thin shells made of FGM compound of stainless steel and nickel. Pradhan *et al.* (2000) extended this work to the case of FGM cylindrical thin shells under various boundary conditions. Ng *et al.* (2001) studied the parametric resonance or dynamic stability of FGM cylindrical thin shells under periodic axial loading. Woo and Meguid (2001) gave an analytical solution for large deflection of thin FGM plates and shallow shells. In their studies the thermal load considered arises from the one dimensional steady heat conduction in the plate thickness direction, but the material properties are temperature independent. Shen (2003) presented a post-buckling analysis for a functionally graded cylindrical thin shell of finite length subjected to external pressure and thermal environments. Yang and Shen (2003) presented a free vibration and parametric resonance of shear deformable functionally graded cylindrical panels. Shahsiah and Eslami (2003) studied thermal buckling of functionally graded cylindrical shell. Sofiyev (2003 and 2004) studied buckling of functionally graded cylindrical shells under different dynamic loading. Based on the high order shear deformation theory, Patel *et al.* (2004) gave the finite element analysis for the free vibration of FGM elliptical cylindrical shell. Shen and Noda (2005) presented post-buckling of a shear deformable FGM cylindrical shell of finite length subjected to combined axial and radial mechanical loads in thermal environments. Yang et al. (2006) presented thermo-mechanical post-buckling of FGM cylindrical panels with temperature-dependent properties that are made of FGMs with temperature dependent thermo-elastic properties that are graded in direction of thickness according to a simple power law distribution in terms of volume fractions of the constituents.

For buckling analysis of isotropic cylindrical shells under external pressure, axial compressive load and torsional load a simple formula for critical buckling loads was given by Mises (1929), Donnell (1934a) and Donnell (1934b), respectively. In addition, there is much literature on vibration (Weingarten 1964, Warburton 1965, Leissa 1973, Chung 1981, Lam and Loy 1995, and Liew *et al.* 2002) and stability analysis of isotropic and composite cylindrical shells under external pressure (Lei and Cheng 1969, Kardomateas 1993, Vodenitcharova and Ansourian 1996, Mirfakhraei and Redekop 1998, Pinna and Ronalds 2000, Xue and Fatt 2002), under axial compressive load (Jones and Morgan 1975, Sheinman *et al*. 1983, Babic and Kilin 1985, Simitses and Anastasiadis 1991, Kardomateas 1993, 1995, Mandal and Calladine 2000, Shen 2002) and under torsional load (Chandrasekaran 1977, Pelekh and Mamchur 1978, Vinson and Sierakowski 1986, Tabiei and Simitses 1994, Kim *et al*. 1999, Tan 2000, Park *et al*. 2001, Mao and Lu 2002).

Several investigations of FGM laminated plates and panels have also been reported. To achieve the active control of the static and dynamic response of FGM shells, Reddy and Cheng (2001), He *et al.* (2002), Liew *et al.* (2002), and Ng *et al.* (2002) used the piezoelectric materials as the integrated sensors/actuators. Lu *et al.* (2005) derived the exact solutions of a simply supported functionally graded piezoelectric plate/laminate under cylindrical bending. Ramirez *et al.* (2006) studied an approximate solution for the static analysis of three-dimensional, anisotropic, elastic plates composed of functionally graded materials (FGM). The solution is obtained by using a discrete layer theory in combination with the Ritz method in which the plate is divided into an arbitrary number of homogeneous and/or FGM layers.

However, the literature on the investigation of vibration and stability problems of composite structures that composed of ceramic, FGM, and metal layers is scarce. A self-consistent constitutive

framework is proposed to describe the behaviour of a generic three-layered system containing a FGM layer subjected to thermal loading given by Pitakthapanaphong and Busso (2002). Frequency characteristics of such a structure were analyzed via the finite element modeling. Analytical solutions of vibration of FGM composite shells with embedded actuating and magnetostrictive layers by using the first-order shear deformation theory are presented by Pradhan and Reddy (2004) and Pradhan (2005), respectively. Kitipornchai *et al*. (2004) further evaluated the sensitivity of the nonlinear vibration characteristics of FGM plates to the initial geometric imperfection of arbitrary shape. Na and Kim (2006) investigated three dimensional thermo-mechanical buckling analysis for FG composite plates that composed of ceramic, FGM, and metal layers by using the finite element methods. Liew *et al*. (2006) presented the non-linear vibration analysis for layered cylindrical panels containing FGMs and subjected to a temperature gradient arising from steady heat conduction through the panel thickness. Kitipornchai *et al*. (2006) investigated the random free vibration of FG laminates with general boundary conditions and subjected to a temperature change, taking into account the randomness in a number of independent input variables such as Young's modulus, Poisson's ratio and thermal expansion coefficient of each constituent material. Sofiyev *et al.* (2006) studied vibration and stability of generic three-layered truncated conical shell containing a FG layer subjected to axial compressive load.

The vibration and stability problems of composite cylindrical shells that composed of ceramic, FGM, and metal layers subjected to various loads have not been studied yet. Therefore, it is very important to develop an accurate, reliable analysis towards the understanding of the stability and vibration characteristics of the layered FGM structures.

This study presents the vibration and stability of composite cylindrical shells that composed of ceramic, FGM, and metal layers subjected to various loads.

2. Formulation of the problem

Fig. 1(a) shows a composite cylindrical shell with simply supported edge conditions, composed of ceramic, FGM, and metal layers, of length L, radius R and total thickness $h = h_1 + h_2$. The ceramic and metal layers are assumed to be homogeneous and isotropic. The shell is referred to a coordinate system xyz in which x and y is in the axial and circumferential directions of the shell and z is in the

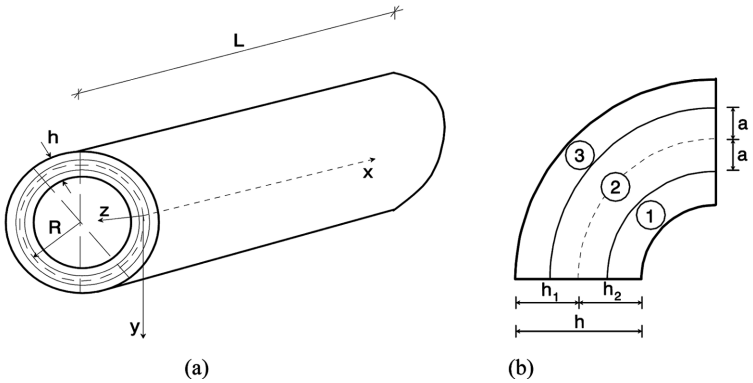

Fig. 1 Schematic representation of (a) a three layered cylindrical shell and coordinate axes, (b) dimensions of the three-layered system

direction of the inward normal to the middle surface.

The in plane geometry of the layered structure is shown in Fig. 1(b). The FGM layer extends from $z = -a$ to $z = +a$ and, for continuous property assumptions to be valid; the thickness of this layer must be significantly larger than dominant micro structural length scale (e.g., grain size). The interfaces between the different layers are assumed to be perfectly bonded at all times and the multilayer system behaviour to be linear elastic.

We assume that the composition is varied from the bottom to top surface, i.e., the bottom surface ($z = -a$) of the layer is metal-rich whereas the top surface ($z = a$) is ceramic-rich. In such a way, the effective material properties P, like Young's modulus E or Poisson's ratio or mass density ρ, can be expressed as

$$P = P_c V_c + P_m V_m \tag{1}$$

in which P_c and P_m denote the temperature-dependent properties of the ceramic and metal surfaces of the FG layer, respectively, and may be expressed as a function of temperature

$$P = P_0(P_{-1}T^{-1} + 1 + P_1 T + P_2 T^2 + P_3 T^3) \tag{2}$$

where P_0, P_{-1}, P_1, P_2 and P_3 are the coefficients showing the temperature-dependency in material properties and are unique to the constituent materials, $T(K)$ is the environment temperature (Touloukian 1967).

V_c and V_m are the ceramic and metal volume fractions of the FG layer and are related by

$$V_c + V_m = 1 \tag{3}$$

Following Reddy and his co-workers, the ceramic volume fraction V_c is assumed as

$$V_c = \left(\frac{z + a}{2a}\right)^N \tag{4}$$

where N is the volume fraction index $0 \le N \le \infty$.

V_c is satisfying the following conditions at the homogeneous layers interfaces (Pitakthapanaphong and Busso 2002),

$$V_c = \begin{cases} 0 & \text{at } z = -a \\ 1 & \text{at } z = a \end{cases} \tag{5}$$

Variation of volume fraction V_c in the thickness direction of composite cylindrical shell composed of Ceramic-FGM-Metal layers is shown in Fig. 2. The top surface is purely ceramic, the middle surface is FGM and bottom surface is fully metal. The horizontal-axis stands for the volumetric percentage of ceramic while vertical-axis represents the position along the thickness of shell. Metal is the dominant constituent at the bottom layer and its volume fraction is increased continually from the bottom to the top of FGM layer. At the top layer, ceramic is the dominant constituent.

From Eqs. (1)-(5), the Young's modulus $\hat{E}$, the Poisson's ratio $\hat{\nu}$ and the mass density $\hat{\rho}$ of an FGM layer can be written as

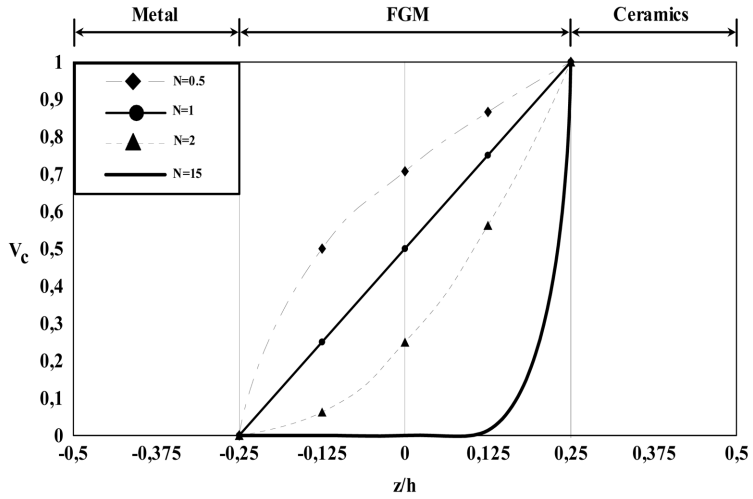

Fig. 2 Variation of volume fraction V_c in thickness direction of the Ceramic-FGM-Metal three layered shell

$$\hat{E} = (E_c - E_m)V_c + E_m \tag{6}$$

$$\hat{\nu} = (\nu_c - \nu_m)V_c + \nu_m \tag{7}$$

$$\hat{\rho} = (\rho_c - \rho_m)V_c + \rho_m \tag{8}$$

where E_m, ν_m, ρ_m and E_c, ν_c, ρ_c are the Young's modulus, Poisson's ratio and density of the metal and ceramic surfaces of the FG layer, respectively.

In the majority of practical applications involving FGMs, they are used as interlayer between two homogeneous materials. For such cases, the through-thickness variation of the Young's modulus, Poisson's ratio and density in the three-layered system are

$$E(\bar{z}) = \begin{cases} E_{0m} & \text{for} \quad -h_1 \le z \le -a \\ E_m + (E_c - E_m)V_c & \text{for} \quad -a \le z \le a \\ E_{0c} & \text{for} \quad a \le z \le h_2 \end{cases} \tag{9.1}$$

$$\nu(\bar{z}) = \begin{cases} \nu_{0m} & \text{for} \quad -h_1 \le z \le -a \\ \nu_m + (\nu_c - \nu_m)V_c & \text{for} \quad -a \le z \le a \\ \nu_{0c} & \text{for} \quad a \le z \le h_2 \end{cases} \tag{9.2}$$

$$\rho(\bar{z}) = \begin{cases} \rho_{0m} & \text{for} \quad -h_1 \le z \le -a \\ \rho_m + (\rho_c - \rho_m)V_c & \text{for} \quad -a \le z \le a \\ \rho_{0c} & \text{for} \quad a \le z \le h_2 \end{cases} \tag{9.3}$$

where E_{0m}, ν_{0m}, ρ_{0m} and E_{0c}, ν_{0c}, ρ_{0c} are the Young's modulus, Poisson's ratio and density of the homogeneous metal and ceramic materials, respectively.

According to the shell theory, the stress-strain relations for thin layered shells are given as follows

$$\begin{Bmatrix} \sigma_x^{(k)} \\ \sigma_y^{(k)} \\ \sigma_{xy}^{(k)} \end{Bmatrix} = \begin{bmatrix} Q_{11}^{(k)} & Q_{12}^{(k)} & 0 \\ Q_{12}^{(k)} & Q_{11}^{(k)} & 0 \\ 0 & 0 & Q_{66}^{(k)} \end{bmatrix} \begin{Bmatrix} e_x - zw_{,xx} \\ e_y - zw_{,yy} \\ e_{xy} - zw_{,xy} \end{Bmatrix} \tag{10}$$

where $\sigma_x^{(k)}, \sigma_y^{(k)}$ and $\sigma_{xy}^{(k)}$ are the stresses in the layers, e_x and e_y are the normal strains in the curvilinear coordinate directions x and y on the middle surface, respectively, whereas e_{xy} is the corresponding shear strain; w is the displacement of the middle surface in the normal direction, positive towards the axis of the cylinder and assumed to be much smaller than the thickness, a comma denotes partial differentiation with respect to the corresponding coordinates.

The quantities $Q_{ij}^{(k)}$, $i,j = 1,2,6$; $k = 1,2,3$ for lamina are

$$Q_{11}^{(1)} = Q_{22}^{(1)} = \frac{E_{0m}}{1-\nu_{0m}^2}, \quad Q_{12}^{(1)} = \frac{\nu_{0m}E_{0m}}{1-\nu_{0m}^2}, \quad Q_{66}^{(1)} = \frac{E_{0m}}{1+\nu_{0m}} \tag{11.1-11.3}$$

$$Q_{11}^{(2)} = Q_{22}^{(2)} = \frac{(E_c - E_m)V_c + E_m}{1-[(\nu_c - \nu_m)V_c + \nu_m]^2} \tag{11.4-11.5}$$

$$Q_{12}^{(2)} = \frac{[(E_c - E_m)V_c + E_m][(\nu_c - \nu_m)V_c + \nu_m]}{1-[(\nu_c - \nu_m)V_c + \nu_m]^2} \tag{11.6}$$

$$Q_{66}^{(2)} = \frac{(E_c - E_m)V_c + E_m}{1+(\nu_c - \nu_m)V_c + \nu_m} \tag{11.7}$$

$$Q_{11}^{(3)} = Q_{22}^{(3)} = \frac{E_{0c}}{1-\nu_{0c}^2}, \quad Q_{12}^{(3)} = \frac{\nu_{0c}E_{0c}}{1-\nu_{0c}^2}, \quad Q_{66}^{(3)} = \frac{E_{0c}}{1+\nu_{0c}} \tag{11.8-11.10}$$

The well-known force and moment resultants are expressed by Wolmir (1967)

$$[(N_x, N_y, N_{xy}), (M_x, M_y, M_{xy})] = \sum_{k=1}^{3} \int_{z_k}^{z_{k+1}} (1, z)[\sigma_x^{(k)}, \sigma_y^{(k)}, \sigma_{xy}^{(k)}]dz \tag{12}$$

The relations between the forces N_x, N_y, N_{xy} and the Airy stress function $\overline{\psi} = \psi/h$ are given by

$$\{N_x, N_y, N_{xy}\} = \{\psi_{,yy}, \psi_{,xx}, -\psi_{,xy}\} \tag{13}$$

For a thin shell, after imposing the following three assumptions about the nonlinear terms: All nonlinear terms not related to the forces N_x^0, N_y^0, N_{xy}^0 are neglected; all nonlinear terms not related to w or its derivatives are neglected; all nonlinear terms not in the dynamic stability and compatibility equations of a shell are neglected (Wolmir 1967).

When the above assumptions are taken into consideration, the modified Donnell type dynamic stability and compatibility equations of composite cylindrical shells that composed of ceramic, FGM, and metal layers are given respectively by

$$\frac{\partial^2 M_x}{\partial x^2} + 2\frac{\partial^2 M_{xy}}{\partial x \partial y} + \frac{\partial^2 M_y}{\partial y^2} + \frac{N_y}{R} + N_x^0 \frac{\partial^2 w}{\partial x^2} + 2N_{xy}^0 \frac{\partial^2 w}{\partial x \partial y} + N_y^0 \frac{\partial^2 w}{\partial y^2} = \rho_t \frac{\partial^2 w}{\partial t^2} \tag{14}$$

$$\frac{\partial^2 e_x}{\partial y^2} + \frac{\partial^2 e_y}{\partial x^2} - 2\frac{\partial^2 e_{xy}}{\partial x \partial y} = -\frac{1}{R}\frac{\partial^2 w}{\partial x^2} \tag{15}$$

where M_x, M_{xy}, M_y are moment resultants, N_x^0, N_y^0 and N_{xy}^0 are the membrane forces for the condition with zero initial moments in the x and y directions and on the xy-plane of the reference surface, respectively, and the mass density per unit length defined as

$$\rho_t = \rho_{0m}(h_1 - a) + \int_{-a}^{a}[(\rho_c - \rho_m)V_c + \rho_m]dz + \rho_{0c}(h_2 - a) \tag{16}$$

Substituting expressions (9-13) and (16) in Eqs. (14) and (15) a system of differential equations for the stress function and the normal displacement can be obtained in form as

$$\begin{aligned} L_{11}\psi + L_{12}w &= 0 \\ L_{21}\psi + L_{22}w &= 0 \end{aligned} \tag{17}$$

where the following definitions apply

$$L_{11} = A_2\left(\frac{\partial^4}{\partial x^4} + \frac{\partial^4}{\partial y^4}\right) + 2(A_1 - A_5)\frac{\partial^4}{\partial x^2 \partial y^2} + \frac{1}{R}\frac{\partial^2}{\partial x^2} \tag{18.1}$$

$$L_{12} = -A_3\left(\frac{\partial^4}{\partial x^4} + \frac{\partial^4}{\partial y^4}\right) - 2(A_4 + A_6)\frac{\partial^4}{\partial x^2 \partial y^2} + N_x^0\frac{\partial^2}{\partial x^2} + N_y^0\frac{\partial^2}{\partial y^2} + 2N_{xy}^0\frac{\partial^2}{\partial x \partial y} - \rho_t\frac{\partial^2}{\partial t^2} \tag{18.2}$$

$$L_{21} = B_1\left(\frac{\partial^4}{\partial x^4} + \frac{\partial^4}{\partial y^4}\right) + 2(B_2 + B_5)\frac{\partial^4}{\partial x^2 \partial y^2} \tag{18.3}$$

$$L_{22} = \frac{1}{R}\frac{\partial^2}{\partial x^2} - B_4\left(\frac{\partial^4}{\partial x^4} + \frac{\partial^4}{\partial y^4}\right) - 2(B_3 + B_6)\frac{\partial^4}{\partial x^2 \partial y^2} \tag{18.4}$$

in which expressions $A_i, B_i (i = 1 \div 6)$ are defined as follows:

$$\begin{gathered} A_1 = C_{11}B_1 + C_{21}B_2, \quad A_2 = C_{11}B_2 + C_{21}B_1, \quad A_3 = C_{11}B_3 + C_{21}B_4 + C_{12} \\ A_4 = C_{11}B_4 + C_{21}B_3 + C_{22}, \quad A_5 = C_{61}B_5, \quad A_6 = C_{61}B_6 + C_{62}, \quad B_1 = C_{10}D \\ B_2 = -C_{20}D, \quad B_3 = (C_{20}C_{21} - C_{11}C_{10})D, \quad B_4 = (C_{20}C_{11} - C_{21}C_{10})D, \quad B_5 = 1/C_{60} \\ B_6 = C_{61}/C_{60}, \quad D = 1/[(C_{10})^2 - (C_{20})^2] \end{gathered} \tag{19.1)-(19.13}$$

in which expressions C_{1k_1}, C_{2k_1} and $C_{6k_1} (k_1 = 0, 1, 2)$ are defined as follows

$$C_{1k_1} = \frac{E_{0m}}{1 - \nu_{0m}^2}\int_{-h_1}^{-a} z^{k_1}dz + \int_{-a}^{a} z^{k_1}\frac{(E_c - E_m)V_c + E_m}{1 - [(\nu_c - \nu_m)V_c + \nu_m]^2}dz + \frac{E_{0c}}{1 - \nu_{0c}^2}\int_{a}^{h_2} z^{k_1}dz \tag{20.1}$$

$$C_{2k_1} = \int_{-a}^{a} z^{k_1}\frac{[(E_c - E_m)V_c + E_m][(\nu_c - \nu_m)V_c + \nu_m]}{1 - [(\nu_c - \nu_m)V_c + \nu_m]^2}dz + \frac{E_{0m}}{1 - \nu_{0m}^2}\int_{-h_1}^{-a} z^{k_1}dz + \frac{E_{0c}}{1 - \nu_{0c}^2}\int_{a}^{h_2} z^{k_1}dz \tag{20.2}$$

$$C_{6k_1} = \frac{E_{0m}}{1+\nu_{0m}} \int_{-h_1}^{-a} z^{k_1} dz + \int_{-a}^{a} z^{k_1} \frac{(E_c - E_m)V_c + E_m}{1+(\nu_c - \nu_m)V_c + \nu_m} dz + \frac{E_{0c}}{1+\nu_{0c}} \int_{a}^{h_2} z^{k_1} dz \tag{20.3}$$

Eq. (17) are the basic differential equations for the vibration and stability of generic composite cylindrical shells containing a FG layer.

3. Composite cylindrical shells containing a FG layer under various loading conditions

3.1 Composite cylindrical shell containing a FG layer under uniform lateral pressure

The origin of the coordinate system is located at the end of the shell in the middle plane. The simply-supported cylindrical shell is subjected to a uniform lateral pressure P (Fig. 3)

$$N_x^0 = 0, \quad N_y^0 = -RP, \quad N_{xy}^0 = 0 \tag{21}$$

The solution of the system of Eq. (17) is sought as follows

$$w = \xi(t)\sin\frac{m_1 x}{R}\sin\frac{ny}{R}, \qquad \psi = \zeta(t)\sin\frac{m_1 x}{R}\sin\frac{ny}{R} \tag{22}$$

where $m_1 = m\pi R/L$, m is the half wave length in the direction of the x-axis, n is the wave number in the direction of the y-axis, $\xi(t)$ and $\zeta(t)$ are the time dependent amplitudes.

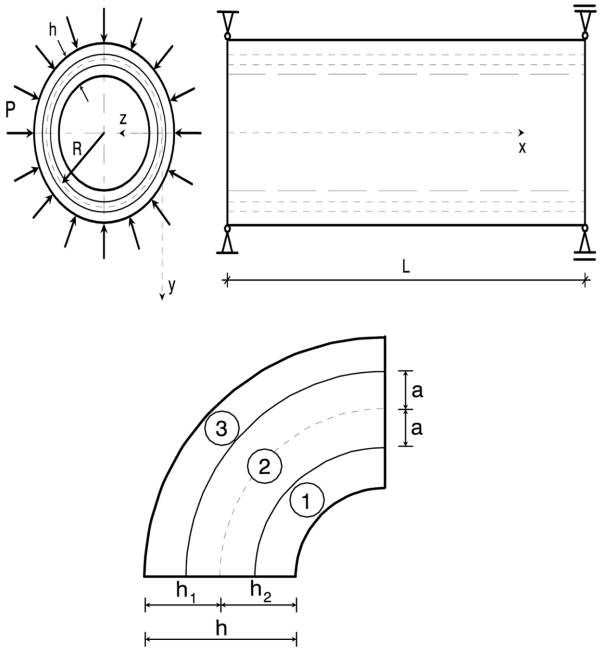

Fig. 3 Composite cylindrical shell containing a FG layer under lateral pressure

Substituting expressions (21) and (22) in the equation set (17), applying Galerkin's method in the ranges $0 \le x \le L$ and $0 \le y \le 2\pi R$ and eliminating $\zeta(t)$ from the equations, the following differential equation is obtained

$$\frac{d^2\xi(t)}{dt^2} + \frac{\Lambda - Pn^2R^{-1}}{\rho_t}\xi(t) = 0 \tag{23}$$

where the following definition apply

$$\Lambda = \frac{1}{R^4}\left\{[A_3(m_1^4 + n^4) + 2(A_4 + A_6)m_1^2n^2] + \right.$$
$$\left.\frac{[m_1^2R - A_2(m_1^4 + n^4) - 2(A_1 - A_5)m_1^2n^2][m_1^2R + B_4(m_1^4 + n^4) + 2(B_3 + B_6)m_1^2n^2]}{B_1(m_1^4 + n^4) + 2(B_2 + B_5)m_1^2n^2}\right\} \tag{24}$$

For the uniform lateral pressure, the following equation is obtained

$$P = \frac{1}{n^2R^3}\left\{[A_3(m_1^4 + n^4) + 2(A_4 + A_6)m_1^2n^2] + \right.$$
$$\left.[m_1^2R - A_2(m_1^4 + n^4) - 2(A_1 - A_5)m_1^2n^2]\frac{[m_1^2R + B_4(m_1^4 + n^4) + 2(B_3 + B_6)m_1^2n^2]}{B_1(m_1^4 + n^4) + 2(B_2 + B_5)m_1^2n^2}\right\} \tag{25}$$

The minimum values of the critical lateral pressure P_{cr} are obtained by minimizing Eq. (25) with respect to m and n, the number of longitudinal and circumferential buckling waves.

When the shell loses stability, lots of short length waves occur around the circumferential direction and (wave length is in $\sqrt{Rh}$ degree) local stability equations can be applied for studying stability. Local stability equations were used when rising zone is smaller than the characteristic parameters of the shell in comparison. But it is proved that it can be applied in general stability loss, which is observed when a half wave occurs along the length of the shell. In certain loading conditions, for example under uniform lateral pressure or torsional load, lots of short waves occur along the circumferential direction. Its mathematical mean is that, according to the circumferential directions of stress and displacement functions, increasing in a derivative is greater than the previous one and the ratio of two derivatives which are consecutive is $\sqrt{R/h}$. In thin shells, $\sqrt{h/R}$ is very small than one, so ψ and w functions may not taken into consideration for the functions which are obtained from their self-derivatives. Its mathematical mean is $n^4 >> (\pi R/L + n\gamma)^4$ and $n^4 >> (\pi R/L)^4$ for torsional load and lateral pressure, respectively. Furthermore, in cylindrical shells that have medium length, the wave number n satisfies the inequality $n\gamma << 1$ for the torsional load (see Sachenkov and Baktieva 1978).

Remembering that when the half wave number m is equal to one, the wave number n for a shell of medium length satisfies the inequality $n^4 >> m_1^4$, for the uniform lateral pressure the following expression is obtained

$$P = \left(\frac{A_3B_1 - A_2B_4}{B_1R^3}\right)n^2 + \frac{\pi^4R^3}{B_1L^4}\frac{1}{n^6} \tag{26}$$

If expression (26) is minimized with respect to the parameter n^2, after some mathematical operations, the following expression is found

$$n_{cr} = \left[\frac{3\pi^4 R^6}{L^4(A_3B_1 - A_2B_4)}\right]^{1/8} \tag{27}$$

Substituting expression (27) in the Eq. (26), the following expression for the minimum values of the critical lateral pressure is obtained

$$P'_{cr} = \frac{4\pi}{3^{3/4}} \times \frac{(A_3B_1 - A_2B_4)^{3/4}}{B_1 R^{3/2} L} \tag{28}$$

3.2 Composite cylindrical shell containing a FG layer under axial compressive load

The origin of the coordinate system is located at the end of the shell in the middle plane. The simply-supported composite cylindrical shell containing a FG layer is subjected to an axial compressive load T (Fig. 4)

$$N_x^0 = -T, \quad N_y^0 = 0, \quad N_{xy}^0 = 0 \tag{29}$$

Substituting expressions (22) and (29) in the equation set (17), applying Galerkin's method in the ranges $0 \le x \le L$ and $0 \le y \le 2\pi R$ and eliminating $\zeta(t)$ from the equations, the following differential equation is obtained:

$$\frac{d^2\xi(t)}{dt^2} + \frac{\Lambda - Tm_1^2 R^{-2}}{\rho_t}\xi(t) = 0 \tag{30}$$

For the axial load, the following equation is obtained

$$T = \frac{1}{m_1^2 R^2}\left\{[A_3(m_1^4 + n^4) + 2(A_4 + A_6)m_1^2 n^2] + \right.$$
$$\left.[m_1^2 R - A_2(m_1^4 + n^4) - 2(A_1 - A_5)m_1^2 n^2] \times \frac{[m_1^2 R + B_4(m_1^4 + n^4) + 2(B_3 + B_6)m_1^2 n^2]}{B_1(m_1^4 + n^4) + 2(B_2 + B_5)m_1^2 n^2}\right\} \tag{31}$$

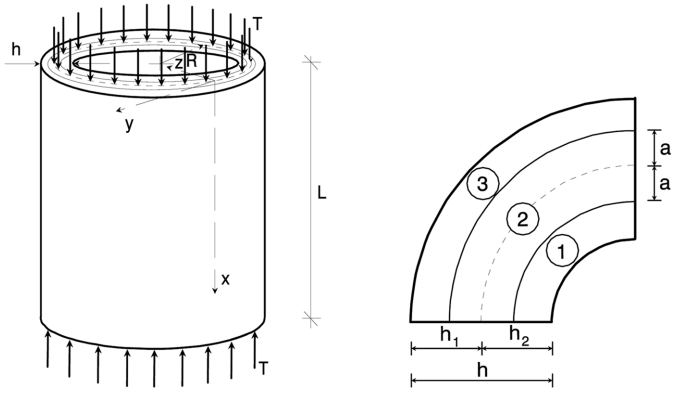

Fig. 4 Composite cylindrical shell containing a FG layer under axial load

The minimum values of the critical axial load T_{cr} are obtained by minimizing Eq. (31) with respect to m and n, the number of longitudinal and circumferential buckling waves.

3.3 Composite cylindrical shell containing a FG layer under Torsional load

The origin of the coordinate system is located at the middle point of the shell in the middle plane. The simply-supported cylindrical shell is subjected to torsional load S (Fig. 5)

$$N_x^0 = 0, \quad N_y^0 = 0, \quad 2N_{xy}^0 = -S \tag{32}$$

The approximate solution to the above-formulated problem is sought in the form (Wolmir 1967)

$$w = \xi(t)\sin\frac{\pi x}{L}\sin\frac{n(y+\gamma x)}{R}, \qquad \psi = \zeta(t)\sin\frac{\pi x}{L}\sin\frac{n(y+\gamma x)}{R} \tag{33}$$

where, γ tangent of the angle between the waves and x axes.

When $x = \pm L/2$ in expressions (32) and (33), although $W = 0$ and $\psi = 0$ conditions are satisfied, neither simple support nor clamped boundary conditions are satisfied. Both boundary conditions are satisfied when they integrated from 0 to $2\pi R$, if $x = \pm L/2$.

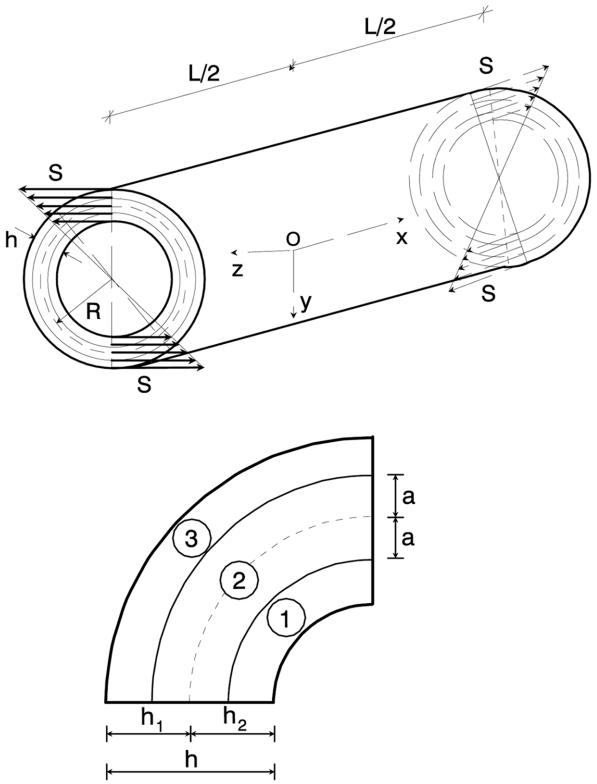

Fig. 5 Three-layered cylindrical shell containing a FG layer under torsional load

Substituting expressions (33) in Eq. (17), then applying Galerkin's method in the ranges $-L/2 \le x \le L/2$ and $0 \le y \le 2\pi R$ and eliminating $\zeta(t)$ from the equations, the following equation is obtained

$$\frac{d^2\xi(t)}{dt^2} + \frac{\Lambda - Sm_1 nR^{-2}}{\rho_t}\xi(t) = 0 \tag{34}$$

For the torsional load, the following equation is obtained

$$S = \frac{1}{m_1 nR^2}\left\{[A_3(m_1^4 + n^4) + 2(A_4 + A_6)m_1^2 n^2] + \right.$$

$$\left.[m_1^2 R - A_2(m_1^4 + n^4) - 2(A_1 - A_5)m_1^2 n^2] \times \frac{[m_1^2 R + B_4(m_1^4 + n^4) + 2(B_3 + B_6)m_1^2 n^2]}{B_1(m_1^4 + n^4) + 2(B_2 + B_5)m_1^2 n^2}\right\} \tag{35}$$

The minimum values of the critical torsional load S_{cr} are obtained by minimizing Eq. (35) with respect to m and n, the number of longitudinal and circumferential buckling waves.

The pre-buckling shear stress in the composite cylindrical shell containing a FG layer can be determined as follows

$$M_{cr} = 2\pi R^2 S_{cr} \tag{36}$$

Remembering that when the half wave number m is equal to one, the wave number n for a shell of medium length satisfies the inequality $n^4 >> (\pi R/L + n\gamma)^4$, for the torsional load the following equation is obtained

$$S = \frac{(A_3B_1 - A_2B_4)L}{B_1\pi R^3}n^3 + \frac{\pi^3 R^3}{L^3 B_1}\frac{1}{n^5} \tag{37}$$

If expression (37) is minimized with respect to the parameter n, after some mathematical operations, the following expression is found

$$n_{cr} = [(5/3)\pi^4 R^6 L^{-4}(A_3B_1 - A_2B_4)^{-1}]^{1/8} \tag{38}$$

Substituting expression (38) in the Eq. (37), the following expression for the minimum values of the critical torsional load is obtained

$$S'_{cr} = 1.6\left(\frac{5}{3}\right)^{3/8}\pi^{1/2} \times L^{-1/2}B_1^{-1}R^{-3/4}(A_3B_1 - A_2B_4)^{5/8} \tag{39}$$

The pre-buckling shear stress in the composite cylindrical shell containing a FG layer can be determined as follows

$$M' = 2\pi R^2 S'_{cr} = 21.581 \times L^{-1/2}B_1^{-1}R^{5/4}(A_3B_1 - A_2B_4)^{5/8} \tag{40}$$

3.4 Free vibration of the composite cylindrical shell containing a FG layer

When $P = 0, T = 0, S = 0$, from Eqs. (23), (30) and (34) for the dimensionless frequency

parameter of free vibration, the following expression is obtained

$$\overline{\omega} = \omega R\sqrt{(1-\nu_{0c}^2)\rho_{0c}/E_{0c}} \tag{41}$$

where the following definition apply

$$\omega = \sqrt{\Lambda/\rho_t} \tag{42}$$

The minimum values of the dimensionless frequency parameter are obtained by minimizing Eq. (41) with respect to m and n, the number of waves.

When $N = 0$ the appropriate formulas for an isotropic cylindrical shell subjected external pressure, axial and torsional loads is found in a special case.

4. Numerical results and discussions

4.1 Comparison results

The numerical results are compared with the previous works to demonstrate the performance of the present study. First, the dimensionless frequency parameter $\omega_1 = \omega L^2(\rho/E_2h^2)^{0.5}/(2\pi)$ and buckling loads for simply supported, single-layer orthotropic and (0°/90°/0°) cross-ply laminated graphite/epoxy circular cylindrical shells under pure axial load and pure uniform lateral pressure are compared in Table 1 with results of the Jones and Morgan (1975), using their material properties, i.e., $E_1 = 30 \times 10^6$ psi; $E_2 = 0.75 \times 10^6$ psi; $G_{12} = 0.375 \times 10^6$ psi; $\nu_1 = 0.25$; $\nu_2 = 0.0625$, and shell parameters $L = 34.64$ in; $R = 10.0$ in; $h = 0.12$ in. It can be seen that the present results are in very good agreement with results of Jones and Morgan (1975).

In addition, the buckling loads for simply supported, isotropic cylindrical shells subjected to uniform lateral pressure are compared in Table 2 with results of Vodenitcharova and Ansourian (1996) and Shen (2003). Clearly, the comparison is excellent and the minor discrepancy is attributed to the difference between the present and other results.

Present results are compared with those presented by Vinson and Sierakowski (1986) and Tan (2000) for isotropic and laminated cylindrical shells under torsion (Table 3). For comparison, the prediction for these loads obtained using the following approximate formula,

$$M_1 = 21.75D_{22}^{5/8}\left(\frac{A_{11}A_{22}-A_{12}^2}{A_{22}}\right)^{3/8}\frac{R^{5/4}}{L^{1/2}} \tag{41}$$

Table 1 Comparisons of dimensionless buckling loads and frequency parameter for single-layer orthotropic and (0°/90°/0°) cross-ply laminated cylindrical shells

	Jones and Morgan (1975)			Present study		
Lay-up	$T_{cr}L^2/E_2h^3$	$P_{cr}RL^2/E_2h^3$	ω_1	$T_{cr}L^2/E_2h^3$	$P_{cr}RL^2/E_2h^3$	ω_1
(0°)	1482	55.90	142.43	1482.0 (3,7)	55.90(1,6)	142.43 (1,5)
(0°/90°/0°)	1859.8	99.39	164.66	1859.8 (3,6)	99.39 (1,5)	164.66 (1,4)

Table 2 Comparisons of buckling loads for isotropic cylindrical shells under uniform lateral pressure ($E=2\times10^{11}$ N/m^2; $\nu=0.3$)

		Shen (2003)	Vodenitcharova and Ansourian (1996)	Present study
L/R	R/h		$P_{cr}\times10^4$ (MPa)	
0.5	300	2761.397 (1,15)	2766.2 (1,15)	2769.014(1,15)
	3000	7.8184 (1.28)	7.816(1,28)	7.821589(1,28)
1	300	1272.597(1,11)	1269.6(1,11)	1273.504(1,11)
	500	348.588 (1,13)	348.43 (1,13)	349.4464(1,13)
	1000	60.5364 (1,15)	60.488 (1,15)	60.59948(1,15)
	1500	21.7969 (1,17)	21.767 (1.17)	21.80382(1,17)
	2000	10.5690 (1,18)	10.559 (1,18)	10.57349(1,18)
	3000	3.8144 (1,20)	3.810 (1,20)	3.815286(1,20)
2	300	611.7448(1,8)	607.33(1,8)	611.7994(1,8)
	3000	1.8842 (1,14)	1.884 (1,14)	1.888939(1,14)
3	300	402.6016 (1,7)	407.19 (1,7)	412.6221(1,7)
	3000	1.2511(1,12)	1.251 (1,12)	1.256187(1,12)
5	300	239.0987(1,5)	235.34 (1,5)	239.4282(1,5)
	3000	0.7482(1,9)	0.744 (1,9)	0.748439(1,9)

The number in brackets indicates the buckling mode (m, n).

Table 3 Comparisons of buckling loads for isotropic and laminated cylindrical shells under torsion ($N\times m$) ($E=10^{11}$ N/m^2; $\nu=0.3$ and $E_1=10^{11}$ N/m^2, $E_2=2\times10^{10}$ N/m^2, $\nu_1=\nu_2=0.3$; $G_{12}=G_{22}=8.5\times10^9$ N/m^2; $R=0.1$ m; $L=0.5$ m)

Thickness h (m)	Material property	Vinson and Sierakowski (1986)	Present study	Tan (2000)
		M_1 ($N\times m$)	$M_{cr}(M'_{cr})$ ($N\times m$)	M_2 ($N\times m$)
0.00001	Isotropic material	0.2183	0.2166(0.2188)	0.2092
	Cross-ply laminates	0.08215	0.07922(0.0790)	0.0713
0.0005	Isotropic material	1451.3	1440.0(1494.0)	1448.0
	Cross-ply laminates	546.15	526.64(516.64)	530.95

which was given by Vinson and Sierakowski (1986). Here, the following definitions apply

$$A_{11}=\frac{E_1h_1}{1-\nu_1\nu_2},\quad A_{22}=\frac{E_2h_1}{1-\nu_1\nu_2},\quad A_{12}=\frac{\nu_2E_1h_1}{1-\nu_1\nu_2},\quad D_{22}=\frac{E_2h_1^3}{12(1-\nu_1\nu_2)} \tag{42}$$

This quantity is also calculated and recorded in Table 3. The values in present study are calculated with Eq. (36) and here values in parentheses are calculated with Eq. (40). The values in Vinson and Sierakowski (1986) are calculated with Eq. (41). It is obvious that good agreement is achieved for all cases.

Besides, to verify the present analysis, our results are compared with those presented by Mao and

Table 4 Critical shear stress (MPa) (wave number) of torsional buckling of some short and long shells ($E = 14 \times 10^9$ N/m^2; $\nu = 0.3$; $h = 0.001$ m)

R/h	*L/R*	Mao and Lu (2002)	Kim *et al.* (1999)	Present study
100.5	4.02	17.41(6)	17.37(6)	16.916(4) *17.258(4)*
100.5	10.05	11.17(4)	11.07(4)	10.699(3) *12.925(3)*
20.5	4.098	125.95(4)	125.57(4)	122.22(3) *144.81(3)*
20.5	10.24	80.38(3)	79.25(3)	77.32(2) *95.40(2)*

Table 5 Comparisons of dimensionless frequency parameter $\overline{\omega} = \omega R\sqrt{(1-\nu_{12}^2)\rho/E_2}$ for a (0°/90°/0°) simply supported laminated cylindrical shell ($R/h = 500$, $L/R = 5$)

(*m*,*n*)	Lam and Loy (1995)	Liew *et al.* (2002)	Present
(1,3)	0.0551	0.0551	0.0566
(1,4)	0.0338	0.0338	0.0337
(1,5)	0.0258	0.0258	0.02556
(1,6)	0.0259	0.0259	0.02559

Lu (2002) and Kim*et al.* (1999) for the homogeneous cylindrical shells under torsion (Table 4). It is obvious that good agreement is achieved for all cases. The values in present study are calculated with Eq. (36) and here the italic numbers are calculated with Eq. (40).

In addition, to verify the present analysis, our results for non-dimensional frequency parameter are compared with those presented by Lam and Loy (1995) and Liew *et al.* (2002) for the homogeneous cross-ply laminated cylindrical shells of lamination scheme (0°/90°/0°). The comparisons for the shell with the following homogeneous material properties: $E_1 = 2.5E_2$, $E_2 = 7.6 \times 10^9$ N/m^2, $\nu_{12} = 0.26$, $\rho = 1643$ kg/m^3 are presented in Table 5. It is obvious that good agreement is achieved for all cases.

4.2 Buckling and vibration results

Numerical results are presented in this section for three layered cylindrical shells containing FG layer with two constituent materials. Two sets of material mixture are considered. One is Silicon nitride and Nickel, referred to as Si_3N_4/Ni or FGM A, and the other is Zirconium oxide and Titanium alloy, referred to as ZrO_2/Ti-6Al-4V or FGM B. The layers of the cylindrical shells include the materials in arrangement as follows: Si_3N_4-FGM A-Ni and ZrO_2-FGM B-Ti-6Al-4V. Typical values Si_3N_4, Ni, ZrO_2 and Ti-6Al-4V are listed in Table 6 (from Reddy and Chin 1998, Kitipornchai *et al.* 2004).

Fig. 6 shows the variations of the dimensionless Young's modulus $\hat{E}/E_m = 1 + (E_c/E_m - 1)V_c$ for $-0.5 \le z/(2a) \le 0.5$ in dimensionless thickness direction $z/(2a)$ for FGM layer with different values of N (see Eq. 6).

Table 6 Temperature-dependent coefficients for ceramics and metals, from Reddy and Chin (1998) and Kitipornchai *et al*. (2004)

Si_3N_4/Nickel (FGM A)						
Coefficients	Silicon nitride (Si_3N_4)			Nickel (Ni)		
	E (Pa)	ν	ρ (kg/m^3)	E (Pa)	ν	ρ (kg/m^3)
P_0	3.4843×10^{11}	0.24	2370	2.2395×10^{11}	0.31	8900
P_{-1}	0	0	0	0	0	0
P_1	-3.07×10^{-4}	0	0	-2.794×10^{-4}	0	0
P_2	2.160×10^{-7}	0	0	-3.998×10^{-9}	0	0
P_3	-8.946×10^{-11}	0	0	0	0	0
P	3.2227×10^{11}	0.24	2370	2.05098×10^{11}	0.31	8900
ZrO_2/Ti-6Al-4V (FGM B)						
Coefficients	Zirconia (ZrO_2)			Titanium alloy (Ti-6Al-4V)		
	E (Pa)	ν	ρ (kg/m^3)	E (Pa)	ν	ρ (kg/m^3)
P_0	2.4427×10^{11}	0.2882	5680	1.2256×10^{11}	0.2884	4420
P_{-1}	0	0	0	0	0	0
P_1	-1.371×10^{-3}	1.133×10^{-4}	0	-4.586×10^{-4}	-1.121×10^{-4}	0
P_2	1.214×10^{-6}	0	0	0	0	0
P_3	-3.681×10^{-10}	0	0	0	0	0
P	1.68063×10^{11}	0.2980	5680	1.05698×10^{11}	0.2981	4420

*The properties were evaluated at $T = 300$ K.

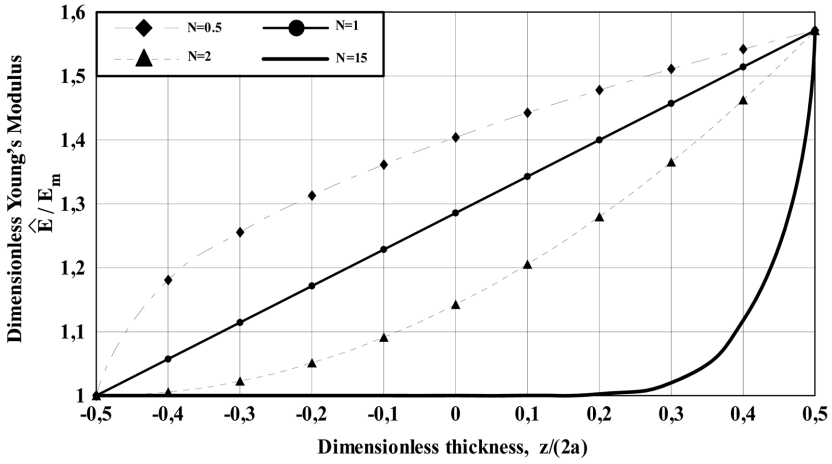

Fig. 6 Variation of the dimensionless Young's modulus in dimensionless thickness direction $z/(2a)$ for FGM layer with different values of N

Tables 7A and 7B indicate the variations of the values of critical loads and dimensionless frequency parameter for composite cylindrical shells composed of Si_3N_4-FGM A-Ni and ZrO_2-FGM B-Ti-6Al-4V layers with R/h ratios.

When the ratio R/h increases, the values of the dimensionless frequency parameter and critical

loads for the composite cylindrical shells composed of Si_3N_4-FGM A-Ni and ZrO_2-FGM B-Ti-6Al-4V layers decrease. When the volume fraction index N increases, the values of the critical loads and the dimensionless frequency parameter decrease from fully ceramic shell to fully metallic shell. When the ratio R/h increases, the increase of the volume fraction index N does not affect the values of the dimensionless frequency parameter and critical loads as the percentage.

Table 7A Variations of the values of critical loads and dimensionless frequency parameter for composite cylindrical shell composed of Si_3N_4-FGM A-Ni layers with ratio R/h ($h/h_1 = h/h_2 = 2$, $h/a = 4$, $L/R = 3$)

	Si_3N_4-FGM A-Ni					
	Si_3N_4	$N = 0.5$	$N = 1$	$N = 2$	$N = 15$	Ni
R/h	P_{cr} (MPa) and (m,n)					
200	0.190(1,6)	0.153(1,6)	0.151(1,6)	0.150(1,6)	0.145(1,6)	0.126(1,6)
300	0.070(1,7)	0.057(1,7)	0.056(1,7)	0.055(1,7)	0.054(1,7)	0.047(1,7)
400	0.033(1,7)	0.027(1,7)	0.027(1,7)	0.026(1,7)	0.025(1,7)	0.022(1,7)
500	0.019(1,8)	0.016(1,7)	0.015(1,7)	0.015(1,7)	0.015(1,7)	0.013(1,7)
R/h	P'_{cr} (MPa) and $(1,n_{cr})$					
200	0.184(1,6)	0.151(1,6)	0.149(1,6)	0.147(1,6)	0.143(1,6)	0.122(1,6)
300	0.067(1,7)	0.055(1,7)	0.054(1,7)	0.053(1,7)	0.052(1,7)	0.044(1,7)
400	0.033(1,7)	0.027(1,7)	0.026(1,7)	0.026(1,7)	0.025(1,7)	0.022(1,7)
500	0.019(1,8)	0.015(1,7)	0.015(1,7)	0.015(1,7)	0.014(1,7)	0.012(1,7)
R/h	$T_{cr} \times 10^{-6}$ (N/m) and (m,n)					
200	10.36(12,13)	8.341(12,13)	8.172(8,12)	7.993(6,11)	7.643(2,7)	6.800(8,12)
300	6.907(8,14)	5.560(8,14)	5.448(8,14)	5.329(11,15)	5.095(11,15)	4.534(8,14)
400	5.181(11,17)	4.170(11,17)	4.086(9,16)	3.997(15,18)	3.821(12,17)	3.399(15,18)
500	4.1447(2,9)	3.3361(12,9)	3.2685(2,9)	3.1976(9,17)	3.0567(9,17)	2.7201(2,9)
R/h	$S_{cr} \times 10^{-6}$ (N/m) and (m,n)					
200	2.172(1,6)	1.752(1,5)	1.715(1,5)	1.676(1,5)	1.601(1,5)	1.427(1,5)
300	1.234(1,6)	0.995(1,6)	0.978(1,6)	0.960(1,6)	0.923(1,6)	0.814(1,6)
400	0.887(1,7)	0.717(1,7)	0.708(1,7)	0.698(1,6)	0.667(1,6)	0.588(1,7)
500	0.650(1,7)	0.524(1,7)	0.516(1,7)	0.507(1,7)	0.489(1,7)	0.429(1,7)
R/h	$S'_{cr} \times 10^{-6}$ (N/m) and $(1,n_{cr})$					
200	2.017(1,6)	1.655(1,6)	1.629(1,6)	1.602(1,6)	1.548(1,6)	1.331(1,6)
300	1.215(1,7)	0.997(1,7)	0.981(1,7)	0.965(1,7)	0.933(1,7)	0.802(1,7)
400	0.848(1,7)	0.696(1,7)	0.685(1,7)	0.673(1,7)	0.651(1,7)	0.560(1,7)
500	0.642(1,7)	0.527(1,7)	0.518(1,7)	0.510(1,7)	0.492(1,7)	0.423(1,7)
R/h	$\overline{\omega}$ and (m,n)					
200	0.056(1,5)	0.034(1,5)	0.032(1,5)	0.030(1,5)	0.028(1,5)	0.023(1,5)
300	0.046(1,6)	0.028(1,6)	0.026(1,6)	0.025(1,6)	0.023(1,6)	0.019(1,6)
400	0.039(1,6)	0.024(1,6)	0.023(1,6)	0.021(1,6)	0.020(1,6)	0.016(1,6)
500	0.036(1,6)	0.022(1,6)	0.021(1,6)	0.019(1,6)	0.018(1,6)	0.015(1,6)

Table 7B Variations of the values of critical loads and dimensionless frequency parameter for composite cylindrical shell composed of ZrO_2-FGM B-Ti-6Al-4V layers with ratio R/h ($h/h_1 = h/h_2 = 2$, $h/a = 4$, $L/R = 3$)

	ZrO_2-FGM B-Ti-6Al-4V					
	ZrO_2	$N = 0.5$	$N = 1$	$N = 2$	$N = 15$	Ti-6Al-4V
R/h	P_{cr} (MPa) and $(1,n_{cr})$					
200	0.136(1,6)	0.094(1,6)	0.093(1,6)	0.092(1,6)	0.089(1,6)	0.068(1,6)
300	0.050(1,7)	0.035(1,7)	0.035(1,7)	0.034(1,7)	0.033(1,7)	0.025(1,7)
400	0.024(1,7)	0.017(1,7)	0.016(1,7)	0.016(1,7)	0.016(1,7)	0.012(1,7)
500	0.014(1,7)	0.010(1,7)	0.010(1,7)	0.009(1,7)	0.009(1,7)	0.007(1,7)
R/h	P'_{cr} (MPa) and $(1,n_{cr})$					
200	0.131(1,6)	0.091(1,6)	0.090(1,6)	0.089(1,6)	0.086(1,6)	0.066(1,6)
300	0.048(1,7)	0.033(1,7)	0.033(1,7)	0.032(1,7)	0.031(1,7)	0.024(1,7)
400	0.023(1,7)	0.016(1,7)	0.016(1,7)	0.016(1,7)	0.015(1,7)	0.012(1,7)
500	0.013(1,7)	0.009(1,7)	0.009(1,7)	0.009(1,7)	0.009(1,7)	0.007(1,7)
R/h	$T_{cr} \times 10^{-6}$ (N/m) and (m,n)					
200	7.365(8,12)	5.062(6,11)	4.970(2,7)	4.874(1,5)	4.684(1,5)	3.695(8,12)
300	4.910(8,14)	3.375(11,15)	3.313(11,15)	3.249(11,15)	3.123(12,15)	2.464(8,14)
400	3.682(15,18)	2.531(15,18)	2.485(12,17)	2.437(12,17)	2.342(8,15)	1.848(15,18
500	2.946(2,9)	2.025(9,17)	1.988(9,17)	1.949(11,18)	1.874(11,18)	1.478(2,9)
R/h	$S_{cr} \times 10^{-6}$ (N/m) and (m,n)					
200	1.546(1,5)	1.064(1,5)	1.039(1,5)	1.008(1,5)	0.969(1,5)	0.776(1,5)
300	0.880(1,6)	0.608(1,6)	0.596(1,6)	0.582(1,6)	0.561(1,6)	0.442(1,6)
400	0.635(1,7)	0.440(1,7)	0.433(1,6)	0.420(1,6)	0.404(1,6)	0.319(1,7)
500	0.464(1,7)	0.321(1,7)	0.315(1,7)	0.308(1,7)	0.297(1,7)	0.233(1,7)
R/h	$S'_{cr} \times 10^{-6}$ (N/m) and (m,n)					
200	1.439(1,6)	0.995(1,6)	0.976(1,6)	0.952(1,6)	0.918(1,6)	0.722(1,6)
300	0.867(1,6)	0.600(1,6)	0.588(1,6)	0.573(1,6)	0.553(1,6)	0.435(1,6)
400	0.605(1,7)	0.419(1,7)	0.410(1,7)	0.400(1,7)	0.386(1,7)	0.304(1,7)
500	0.458(1,7)	0.317(1,7)	0.310(1,7)	0.303(1,7)	0.292(1,7)	0.230(1,7)
R/h	$\overline{\omega}$ and (m,n)					
200	0.055(1,5)	0.048(1,5)	0.048(1,5)	0.048(1,5)	0.048(1,5)	0.044(1,5)
300	0.046(1,6)	0.040(1,6)	0.040(1,6)	0.040(1,6)	0.040(1,6)	0.037(1,6)
400	0.039(1,6)	0.034(1,6)	0.034(1,6)	0.034(1,6)	0.034(1,6)	0.031(1,6)
500	0.036(1,6)	0.031(1,6)	0.031(1,6)	0.031(1,6)	0.031(1,6)	0.029(1,6)

Variation of the ratio R/h affects more to the values of critical lateral pressure, and less to the critical torsional load, and the least to the values of the axial load.

When the ratio $R/h = 500$, the difference between the values of P_{cr} and P'_{cr} changes between 1.37%-2.5%; the difference between the values of S_{cr} and S'_{cr} changes between 0.45%-0.78% for the composite cylindrical shell composed of Si_3N_4-FGM A-Ni layers.

When the ratio $R/h = 500$, the difference between the values of P_{cr} and P'_{cr} changes between 2.1% -5.6%; the difference between the values of S_{cr} and S'_{cr} changes between 1.25%-1.75% for the composite cylindrical shell composed of ZrO_2-FGM B-Ti-6Al-4V layers.

Consequently, values of the expressions P_{cr} or P'_{cr} and S_{cr} or S'_{cr} are closed each other, respectively. Then, one of the formulations (25) or (28) and (35) or (38) can be used for calculations, respectively.

Furthermore, values of the critical axial loads are importantly bigger than the values of critical torsional loads, and are extreme from the values of critical lateral pressure.

Tables 8A and 8B give the variations of the values of critical loads and dimensionless frequency

Table 8A Variations of the values of critical loads and dimensionless frequency parameter for composite cylindrical shell composed of Si_3N-FGM A-Ni layers with ratio $h/(2a)$ ($h_1 = h_2$, $R/h = 200$, $L/R = 3$)

			Si_3N_4-FGM A-Ni			
	Si_3N_4	$N = 0.5$	$N = 1$	$N = 2$	$N = 15$	Ni
$h/2a$			P_{cr} (MPa) and (m,n)			
1.0		0.155(1,6)	0.146(1,6)	0.139(1,6)	0.124(1,6)	
1.1		0.156(1,6)	0.149(1,6)	0.143(1,6)	0.130(1,6)	
1.5	0.19	0.155(1,6)	0.152(1,6)	0.149(1,6)	0.141(1,6)	0.126
1.9	(1,6)	0.154(1,6)	0.152(1,6)	0.150(1,6)	0.145(1,6)	(1,6)
2.0		0.153(1,6)	0.151(1,6)	0.150(1,6)	0.145(1,6)	
5.0		0.151(1,6)	0.150(1,6)	0.150(1,6)	0.148(1,6)	
$h/2a$			$T_{cr} \times 10^{-6}$ (N/m) and (m,n)			
1.0		8.515(12,13)	8.022(12,13)	7.562(8,12)	6.623(8,12)	
1.1		8.509 (12,13)	8.100(8,12)	7.703(6,11)	6.887(2,7)	
1.5	10.36	8.423 (12,13)	8.175(8,12)	7.920(2,7)	7.397(1,5)	6.80
1.9	(12,13)	8.354 (12,13)	8.173(8,12)	7.984(2,7)	7.609(2,7)	(8,12)
2.0		8.341 (12,13)	8.172(8,12)	7.993(2,7)	7.643(2,7)	
5.0		8.222 (12,13)	8.160(12,13)	8.097(12,13)	7.982(8,12)	
$h/2a$			$S_{cr} \times 10^{-6}$ (N/m) and (m,n)			
1.0		1.775(1,6)	1.677(1,6)	1.587(1,5)	1.388(1,5)	
1.1		1.782(1,6)	1.700(1,5)	1.615(1,5)	1.443(1,5)	
1.5	2.172	1.769(1,5)	1.715(1,5)	1.660(1,5)	1.549(1,5)	1.427
1.9	(1,6)	1.755(1,5)	1.715(1,5)	1.674(1,5)	1.594(1,5)	(1,5)
2.0		1.752(1,5)	1.715(1,5)	1.676(1,5)	1.601(1,5)	
5.0		1.723(1,5)	1.715(1,5)	1.700(1,5)	1.675(1,5)	
$h/2a$			$\overline{\omega}$ and (m,n)			
1.0		0.036(1,5)	0.032(1,5)	0.028(1,5)	0.023(1,5)	
1.1		0.036(1,5)	0.032(1,5)	0.029(1,5)	0.024(1,5)	
1.5	0.056	0.035(1,5)	0.032(1,5)	0.030(1,5)	0.026(1,5)	0.023
1.9	(1,5)	0.034(1,5)	0.032(1,5)	0.030(1,5)	0.027(1,5)	(1,5)
2.0		0.034(1,5)	0.032(1,5)	0.030(1,5)	0.028(1,5)	
5.0		0.033(1,5)	0.032(1,5)	0.031(1,5)	0.030(1,5)	

Table 8B Variations of the values of critical loads and dimensionless frequency parameter for composite cylindrical shell composed of ZrO_2-FGM B-Ti-6Al-4V layers with ratio $h/(2a)$ ($h_1 = h_2$, $R/h = 200$, $L/R = 3$)

			ZrO_2-FGM B-Ti-6Al-4V			
	ZrO_2	$N = 0.5$	$N = 1$	$N = 2$	$N = 15$	Ti-6Al-4V
$h/2a$			P_{cr} (MPa) and (m,n)			
1.0		0.081(1,6)	0.075(1,6)	0.071(1,6)	0.063(1,6)	
1.1		0.086(1,6)	0.082(1,6)	0.079(1,6)	0.072(1,6)	
1.5	0.136	0.093(1,6)	0.091(1,6)	0.089(1,6)	0.085(1,6)	0.068
1.9	(1,6)	0.094(1,6)	0.093(1,6)	0.092(1,6)	0.089(1,6)	(1,6)
2.0		0.094(1,6)	0.093(1,6)	0.092(1,6)	0.089(1,6)	
5.0		0.095(1,6)	0.094(1,6)	0.094(1,6)	0.093(1,6)	
$h/2a$			$T_{cr} \times 10^{-6}$ (N/m) and (m,n)			
1.0		4.397(12,13)	4.104(12,13)	3.849(8,12)	3.390(8,12)	
1.1		4.604(8,12)	4.367(2,7)	4.151(1,5)	3.738(1,5)	
1.5	7.365	4.941(2,7)	4.803(1,5)	4.663(1,5)	4.386(1,5)	3.695
1.9	(8,12)	5.047(2,7)	4.948(2,7)	4.846(1,5)	4.642(1,5)	(8,12)
2.0		5.062(6,11)	4.969(2,7)	4.874(1,5)	4.684(1,5)	
5.0		5.198(12,13)	5.165(12,13)	5.131(12,13)	5.071(8,12)	
$h/2a$			$S_{cr} \times 10^{-6}$ (N/m) and (m,n)			
1.0		0.923(1,5)	0.862(1,5)	0.808(1,5)	0.711(1,5)	
1.1		0.9661,5)	0.915(1,5)	0.869(1,5)	0.783(1,5)	
1.5	1.546	1.035(1,5)	1.006(1,5)	0.977(1,5)	0.919(1,5)	0.776
1.9	(1,5)	1.058(1,5)	1.037(1,5)	1.015(1,5)	0.972(1,5)	(1,5)
2.0		1.062(1,5)	1.041(1,5)	1.021(1,5)	0.981(1,5)	
5.0		1.085(1,6)	1.082(1,6)	1.078(1,6)	1.064(1,6)	
$h/2a$			$\overline{\omega}$ and (m,n)			
1.0		0.044(1,5)	0.044(1,5)	0.043(1,5)	0.042(1,5)	
1.1		0.045(1,5)	0.045(1,5)	0.045(1,5)	0.044(1,5)	
1.5	0.055	0.047(1,5)	0.047(1,5)	0.047(1,5)	0.047(1,5)	0.044
1.9	(1,5)	0.048(1,5)	0.048(1,5)	0.048(1,5)	0.048(1,5)	(1,5)
2.0		0.048(1,5)	0.048(1,5)	0.048(1,5)	0.048(1,5)	
5.0		0.049(1,5)	0.049(1,5)	0.049(1,5)	0.049(1,5)	

parameter for composite cylindrical shell composed of Si_3N_4-FGM A-Ni and ZrO_2-FGM B-Ti-6Al-4V layers with respect to $h/(2a)$ ratios. When $h/(2a) = 1$ the structure is pure FGM shell.

When the ratio $h/(2a)$ increases, the values of the dimensionless frequency parameter and critical loads for the composite cylindrical shells composed of Si_3N_4-FGM A-Ni and ZrO_2-FGM B-Ti-6Al-4V layers increase if $N \geq 1$ and decrease if $0 < N < 1$. On the other hand, when FG layer thickness is increased, the values of the critical loads for the three layered cylindrical shells degrease if $N \geq 1$ and increase if $0 < N < 1$. This shows that the purely FGM cylindrical shell is more stable than the FGM composite cylindrical shell which is more stable than the classical ceramic or metal

cylindrical shell if $N \geq 1$. But the purely FG cylindrical shell is more instable than the FG composite cylindrical shell which is more instable than the classical ceramic or metal cylindrical shell if $0 < N < 1$. When the volume fraction index N increases, the values of the critical loads and the dimensionless frequency parameter decrease. When the volume fraction index N increases, the effect to the critical parameters increases. When the ratio $h/(2a)$ increases the effect of the volume fraction index N to the critical parameters increases.

If we compare with the critical parameter values of the composite cylindrical shells composed of Si_3N_4-FGM A-Ni and ZrO_2-FGM B-Ti-6Al-4V layers, critical parameter values are small in type ZrO_2-FGM B-Ti-6Al-4V shell, but the effect of the variation of volume fraction index N to the critical parameter values is more as a percentage. For example; for the composite cylindrical shell composed of Si_3N_4-FGMA-Ni layers, for $h/(2a) = 5$, by comparison with purely FGM A cylindrical

Table 9A Variations of the values of critical loads and dimensionless frequency parameter for composite cylindrical shell composed of Si_3N_4-FGM A-Ni layers with ratio L/R ($h/h_1 = h/h_2 = 2$, $h/a = 4$, $R/h = 300$)

	Si_3N_4-FGM A-Ni					
	Si_3N_4	$N = 0.5$	$N = 1$	$N = 2$	$N = 15$	Ni
L/R	P_{cr} (MPa) and (m,n)					
3	0.070(1,7)	0.057(1,7)	0.056(1,7)	0.055(1,7)	0.054(1,6)	0.047(1,7)
9	0.023(1,4)	0.018(1,4)	0.018(1,4)	0.018(1,4)	0.018(1,4)	0.015(1,4)
15	0.013(1,3)	0.011(1,3)	0.011(1,3)	0.011(1,3)	0.010(1,3)	0.009(1,3)
L/R	P'_{cr} (MPa) and $(1,n_{cr})$					
3	0.067(1,7)	0.055(1,7)	0.054(1,7)	0.053(1,7)	0.052(1,7)	0.044(1,7)
9	0.022(1,4)	0.018(1,4)	0.018(1,4)	0.018(1,4)	0.017(1,4)	0.015(1,4)
15	0.013(1,3)	0.011(1,3)	0.011(1,3)	0.011(1,3)	0.010(1,3)	0.010(1,3)
L/R	$T_{cr} \times 10^{-6}$ (N/m) and (m,n)					
3	6.907(8,14)	5.560(8,14)	5.448(8,14)	5.329(11,15	5.095(11,15	4.53(8,14)
9	6.907(8,9)	5.560(8,9)	5.449(8,9)	5.329(13,11	5.095(13,11	4.53(13,11
15	6.914(13,9)	5.566(13,9)	5.451(8,7)	5.330(8,7)	5.094(8,7)	4.536(8,7)
L/R	$S_{cr} \times 10^{-6}$ (N/m) and (m,n)					
3	1.234(1,6)	0.995(1,6)	0.978(1,6)	0.960(1,6)	0.923(1,6)	0.814(1,6)
9	0.780(1,4)	0.632(1,4)	0.625(1,4)	0.618(1,4)	0.600(1,4)	0.519(1,4)
15	0.576(1,3)	0.466(1,3)	0.460(1,3)	0.454(1,3)	0.441(1,3)	0.383(1,3)
L/R	$S'_{cr} \times 10^{-6}$ (N/m) and $(1,n_{cr})$					
3	1.215(1,6)	0.997(1,6)	0.981(1,6)	0.965(1,6)	0.933(1,6)	0.802(1,6)
9	0.702(1,4)	0.576(1,4)	0.566(1,4)	0.557(1,4)	0.538(1,4)	0.463(1,4)
15	0.544(1,3)	0.446(1,3)	0.439(1,3)	0.432(1,3)	0.417(1,3)	0.356(1,3)
L/R	$\overline{\omega}$ and (m,n)					
3	0.046(1,6)	0.028(1,6)	0.026(1,6)	0.025(1,6)	0.023(1,6)	0.019(1,6)
9	0.016(1,3)	0.010(1,3)	0.009(1,3)	0.009(1,3)	0.008(1,3)	0.006(1,3)
15	0.010(1,3)	0.006(1,3)	0.006(1,3)	0.005(1,3)	0.005(1,3)	0.004(1,3)

Table 9B Variations of the values of critical loads and dimensionless frequency parameter for composite cylindrical shell composed of ZrO_2-FGM B-Ti-6Al-4V layers with ratio L/R ($h/h_1 = h/h_2 = 2$, $h/a = 4$, $R/h = 300$)

	ZrO_2-FGM B-Ti-6Al-4V					
	ZrO_2	$N = 0.5$	$N = 1$	$N = 2$	$N = 15$	Ti-6Al-4V
L/R	P_{cr} (MPa) and (m,n)					
3	0.0501(1,7)	0.0348(1,7)	0.0345(1,7)	0.0342(1,7)	0.0331(1,6)	0.0251(1,7)
9	0.016(1,4)	0.011(1,4)	0.011(1,4)	0.011(1,4)	0.011(1,4)	0.008(1,4)
15	0.010(1,3)	0.007(1,3)	0.007(1,3)	0.007(1,3)	0.006(1,3)	0.005(1,3)
L/R	P'_{cr} (MPa) and $(1,n_{cr})$					
3	0.048(1,7)	0.033(1,7)	0.033(1,7)	0.032(1,7)	0.031(1,7)	0.024(1,7)
9	0.016(1,4)	0.011(1,4)	0.011(1,4)	0.011(1,4)	0.010(1,4)	0.008(1,4)
15	0.010(1,3)	0.007(1,3)	0.007(1,3)	0.007(1,3)	0.006(1,3)	0.005(1,3)
L/R	$T_{cr} \times 10^{-6}$ (N/m) and (m,n)					
3	4.910(8,14)	3.375(11,15)	3.313(11,15)	3.249(11,15)	3.123(12,15)	2.464(8,14)
9	4.910(8,9)	3.375(13,11)	3.313(13,11)	3.250(13,11)	3.125(13,11)	2.464(8,9)
15	4.913(8,7)	3.378(8,7)	3.313(8,7)	3.249(8,7)	3.122(14,9)	2.465(8,7)
L/R	$S_{cr} \times 10^{-6}$ (N/m) and (m,n)					
3	0.880(1,6)	0.607(1,6)	0.598(1,6)	0.589(1,6)	0.568(1,6)	0.442(1,6)
9	0.559(1,4)	0.389(1,4)	0.385(1,4)	0.381(1,4)	0.370(1,4)	0.281(1,4)
15	0.413(1,3)	0.286(1,3)	0.283(1,3)	0.280(1,3)	0.272(1,3)	0.207(1,3)
L/R	$S'_{cr} \times 10^{-6}$ (N/m) and $(1,n_{cr})$					
3	0.867(1,6)	0.599(1,6)	0.590(1,6)	0.581(1,6)	0.560(1,6)	0.435(1,6)
9	0.500(1,4)	0.346(1,4)	0.341(1,4)	0.335(1,4)	0.323(1,4)	0.251(1,4)
15	0.388(1,3)	0.268(1,3)	0.264(1,3)	0.260(1,3)	0.251(1,3)	0.195(1,3)
L/R	$\overline{\omega}$ and (m,n)					
3	0.046(1,6)	0.040(1,6)	0.040(1,6)	0.040(1,6)	0.040(1,6)	0.037(1,6)
9	0.016(1,3)	0.014(1,3)	0.014(1,3)	0.014(1,3)	0.013(1,3)	0.013(1,3)
15	0.010(1,3)	0.009(1,3)	0.009(1,3)	0.009(1,3)	0.009(1,3)	0.008(1,3)

shell, the effect to the critical lateral pressure is 2.79% for $N = 0.5$, and 16.72% for $N = 15$. For the composite cylindrical shell composed of ZrO_2-FGM B-Ti-6Al-4V layers, by comparison with purely FGM B cylindrical shell, the effect to the critical lateral pressure is 14.89% for $N = 0.5$, and 32.05% for $N = 15$. In addition, this is satisfied for axial and torsional loads.

Furthermore, the values of the critical loads and dimensionless frequency parameter of purely FGM shells are under the values of purely metal shells when volume fraction index $N \geq 15$, but values of the critical loads and dimensionless frequency parameter of composite cylindrical shells composed of Si_3N_4-FGM A-Ni and ZrO_2-FGM B-Ti-6Al-4V layers change between the values of fully ceramic and fully metal cylindrical shells.

The influence of aspect ratio L/R on the values of critical loads and dimensionless frequency parameter for composite cylindrical shells composed of Si_3N_4-FGM A-Ni and ZrO_2-FGM B-Ti-6Al-

4V layers are shown in Tables 9A and 9B.

When the ratio L/R increases, the values of the dimensionless frequency parameter and critical loads for the cylindrical shells composed of Si_3N_4-FGM A-Ni and ZrO_2-FGM B-Ti-6Al-4V layers decrease. When the volume fraction index N increases, the values of the critical loads and dimensionless frequency parameter decrease from fully ceramic to fully metallic cylindrical shells. When the ratio L/R increases, the increase of the volume fraction index N does not affect the values of the critical loads and dimensionless frequency parameter as the percentage.

When the ratio L/R increases, the biggest effect is to the values of the critical lateral pressure, and less to the critical torsional load, but the values of the axial load does not change. Minimum values of the critical lateral pressure and torsional loads are obtained from one more of the value of the wave number corresponding to the minimum values of the dimensionless frequency parameter. Critical axial load values are obtained from the big values of wave numbers m and n.

When the ratio $L/R = 3$, the difference between the values of S_{cr} and S'_{cr} changes between 0.25%-0.98% for the shell composed of Si_3N_4-FGM A-Ni layers; when the ratio $L/R = 15$, the difference between the values of P_{cr} and P'_{cr} changes between 0%-0.94%.

When the ratio $L/R = 3$, the difference between the values of S_{cr} and S'_{cr} changes between 0.25%-0.36% for the shell composed of ZrO_2-FGM B-Ti-6Al-4V layers; when the ratio $L/R = 15$, the difference between the values of P_{cr} and P'_{cr} changes between 0%-1.5%. Consequently, one of the formulations (25) or (28) and (35) or (38) can be used for calculation of the expressions P_{cr} or P'_{cr} and S_{cr} or S'_{cr}, respectively (Tables 9A and 9B).

For all cases, the longitudinal wave numbers corresponding to the minimum values of the dimensionless frequency parameter, critical torsional load and critical external pressure are equal to one. Minimum values of the critical lateral pressure and torsional load are obtained from one more of the values of the circumferential wave number corresponding to the minimum values of the dimensionless frequency parameter. Values of the critical axial load are obtained from the big values of wave numbers m and n.

When the critical parameters values of the cylindrical shells composed of Si_3N_4-FGM A-Ni and ZrO_2–FGM B-Ti-6Al-4V layers are compared with each other, it is seen that the critical parameters values of the cylindrical shell composed of ZrO_2-FGM B-Ti-6Al-4V layers are less than the other (see Tables 7-9).

5. Conclusions

In this study, a formulation for the vibration and stability of composite cylindrical shells that composed of ceramic, FGM, and metal layers subjected to various loads is presented. The properties are graded in the thickness direction according to a volume fraction power-law distribution. The modified Donnell type stability and compatibility equations are obtained. Applying Galerkin's method analytic solutions are obtained for the critical loads and free vibration frequency parameter. The detailed parametric studies are carried out to study the influences of thickness variation of the FG layer, radius-to-thickness ratio, lengths-to-radius ratio, material composition and material profile index on the critical parameters of three-layered cylindrical shells. Comparing results with those in the literature validates the present analysis.

The numerical results support the following conclusions:

a) For all compositional profiles, as the ratios R/h and L/R increases the values of the

dimensionless frequency parameter and critical loads for the composite cylindrical shells that composed of ceramic, FGM, and metal layers decrease.

b) When FG layer thickness is increased, the values of the critical loads for the three layered cylindrical shells degrease if $N \geq 1$ and increase if $0 < N < 1$.

c) When the volume fraction index N increases, the effect to the critical parameters increases.

d) The values of the critical loads and dimensionless frequency parameter of purely FG shells are under the values of purely metal shells for large values of the volume fraction index, but values of the critical loads and dimensionless frequency parameter of FG composite cylindrical shells change between the values of fully ceramic and fully metal cylindrical shells.

e) For all cases, the longitudinal wave numbers corresponding to the minimum values of the dimensionless frequency parameter, critical torsional load and critical external pressure are equal to one. Minimum values of the critical lateral pressure and critical torsional load are obtained from one more of the values of the circumferential wave number corresponding to the minimum values of the dimensionless frequency parameter. Values of the critical axial load are obtained from the big values of wave numbers m and n.

References

Babich, I.Y. and Kilin, V.I. (1985), "Stability of a three-layer orthotropic cylindrical shell under axial loading", *Soviet Appl. Mech.*, **21**, 566-669.

Biesheuvel, P.M. and Verweij, H. (2000), "Calculation of the composition profile of a functionally graded material produced by centrifugal casting", *J. Am. Ceram. Soc.*, **83**(4), 743-749.

Birman, V. (1995), "Buckling of functionally graded hybrid composite plates", *In: Proc. 10th Conf. on Eng. Mech., Boulder*, USA.

Chandrasekaran, K. (1977), "Torsional vibrations of some layered shells of revolution", *J. Sound Vib.*, **55**, 27-37.

Chung, H. (1981), "Free vibration analysis of circular cylindrical shells", *J. Sound Vib.*,**74**, 331-350.

Donnell, L.H. (1934a), "Stability of thin-walled tubes under torsion", *NACA Tr*-479.

Donnell, L.H. (1934b), "A new theory for the buckling of the thin cylinders under axial compression and bending", *Trans Asme,* **56**, 795-806.

Feldman, E. and Aboudi, J. (1997), "Buckling analysis of functionally graded plates subjected to uniaxial loading", *Compos. Struct*., **38**, 29-36.

Groves, J.F. and Wadley, H.N.G. (1997), "Functionally graded materials synthesis via low vacuum directed vapor deposition", *Compos. Part. B-Eng.*, **28**(1-2), 57-69.

He, X.Q., Liew, K.M., Ng, T.Y. and Sivashanker, A. (2002), "A FEM model for the active control of curved FGM shells using piezoelectric sensor/actuator layers", *Int. J. Num. Meth. Eng.*, **54**(6), 853-870.

Jones, R.M. and Morgan, H.S. (1975), "Buckling and vibration of cross-ply laminated circular cylindrical shells", *AIAA J.*, **13**(5), 664-671.

Kardomateas, G.A. (1993), "Buckling of thick orthotropic cylindrical shells under external pressure", *J. Appl. Mech*., **60**, 195-2002.

Kardomateas, G.A. (1993), "Stability loss in thick transversely isotropic cylindrical shells under axial compression", *J. Appl. Mech.*, **60**(2), 506-513.

Kardomateas, G.A. (1995), "Bifurcation of equilibrium in thick orthotropic cylindrical shells under axial compression", *J. Appl. Mech.*, **62**(1), 43-52.

Kieback, B., Neubrand, A. and Riedel, H. (2003), "Processing techniques for functionally graded materials", *Mater. Sci. Eng. A-Struct. Material Prop. Micro-Struct. Process*, **362**(1-2), 81-105.

Kim, Y.S., Kardomateas, G.A. and Zureick, A. (1999), "Buckling of thick orthotropic cylindrical shells under torsion", *J. Appl. Mech*., **66**, 41-50.

Kitipornchai, S., Yang, J. and Liew, K.M. (2004), "Semi analytical for nonlinear vibration of laminated FGM

plates with geometric imperfections", *Int. J. Solids Struct.*, **41**, 2235-2257.
Kitipornchai, S., Yang, J. and Liew, K.M. (2006), "Random vibration of the functionally graded laminates in thermal environments", *Comput. Meth. Appl. Mech. Eng.*, **195**, 1075-1095.
Koizumi, M. (1993), "The concept of FGM", *Ceramic Transactions, Functionally Gradient Mater.*, **34**, 3-10.
Lam, K.Y. and Loy, C.T. (1995), "Analysis of rotating laminated cylindrical shells by different thin shell theories", *J. Sound Vib.*, **186**, 23-35.
Lei, M.M. and Cheng, S. (1969), "Buckling of composite and homogeneous isotropic cylindrical shells under axial and radial loading", *J. Appl. Mech.*, 791-798.
Leissa, A.W. (1973), *Vibration of Shells.* NASA SP-288.
Liew, K.M., He, X.Q., Ng, T.Y. and Kitipornchai, S. (2002), "Active control of FGM shell subjected to a temperature gradient via piezoelectric sensor/actuator patches", *Int. J. Num. Meth. Eng.*, **55**, 653-668.
Liew, K.M., Ng, T.Y. and Zhao, X. (2002), "Vibration of axially loaded rotating cross-ply laminated cylindrical shells via ritz method", *J. Eng. Mech.*, **128**(9), 1001-1007.
Liew, K.M., Yang, J. and Wu, Y.F. (2006), "Nonlinear vibration of a coating-FGM-substrate cylindrical panel subjected to a temperature gradient", *Comput. Meth. Appl. Mech. Eng.*, **195**(9-12), 1007-1026.
Loy, C.T., Lam, K.Y. and Reddy, J.N. (1999), "Vibration of functionally graded cylindrical shells", *Int. J. Mech. Sci.*, **41**, 309-324.
Lu, P., Lee, H.P. and Lu, C. (2005), "An exact solution for functionally graded piezoelectric laminates in cylindrical bending", *Int. J. Mech. Sci.*, **47**, 437-458
Mandal, P. and Calladine, C.R. (2000), "Buckling of thin cylindrical shells under axial compression", *Int. J. Solid Struct.*, **37**, 4509-4525.
Mao, R. and Lu, C.H. (1999), "Buckling analysis of a laminated cylindrical shell under torsion subjected to mixed boundary conditions", *Int. J. Solids Struct.*, **36**, 3821-3835.
Mirfakhraei, P. and Redekop, D. (1998), "Buckling of circular cylindrical shells by the differential quadrature method", *Int. J. Pressure Vessels Piping*, **75**, 347-353.
Mises, R. (1929), "Der Kritische Aussendruck Für Allseits Belastete Cylindrisher Rohre, Festscher", *Zum. 70 Geburtstage von prof. A Stodola, Zürich*, 418-432. (Germany)
Mortensen, A. and Suresh, S. (1995), "Functionally graded metals and metal ceramic composites", *I. Proc. Int. Mater. Rev.*, **40**(6), 239-265.
Na, K.S. and Kim, J.H. (2006), "Three-dimensional thermo-mechanical buckling analysis for functionally graded composite plates", *Compos. Struct.* in press
Ng, T.Y., He, X.Q. and Liew, K.M. (2002), "Finite element modeling of active control of functionally graded shells in frequency domain via piezoelectric sensors and actuators", *Comput. Mech.*, **28**(1), 1-9.
Ng, T.Y., Lam, K.Y., Liew, K.M. and Reddy, N.J. (2001), "Dynamic stability analysis of functionally graded cylindrical shells under periodic axial loading", *Int. J. Solids Struct.*, **38**, 1295-1309.
Park, H.C., Cho, C.M. and Choi, Y.H., (2001), "Torsional buckling analysis of composite cylinders", *AIAA J.*, **39**, 951-955.
Patel, B.P., Gupta, M.S., Loknath, M.S. and Kadu, C.P. (2005), "Free vibration analysis of a functionally graded elliptical cylindrical shells using higher-order theory", *Compos. Struct.*, **69**, 259-270.
Pelekh, B.L. and Mamchur, I.L. (1978), "Torsion of the laminated transversal isotropic cylindrical shells", *Soviet Appl. Mech.*, **14**, 24-28.
Pinna, R. and Ronalds, B.F. (2000), "Hydrostatic buckling of shells with various boundary conditions", *J. Constr. Steel. Res.*, **56**(1), 1-16.
Pitakthapanaphong, S. and Busso, E.P. (2002), "Self-consistent elasto-plastic stress solutions for functionally graded material systems subjected to thermal transients", *J. Mech. Phys. Solids*, **50**, 695-716.
Pradhan, S.C. (2005), "Vibration suppression of FGM composite shells using embedded magnetostrictive layers", *Int. J. Solids Struct.*, **42**, 2465-2488.
Pradhan, S.C. and Reddy, J.N. (2004), "Vibration control of composite shells using embedded actuating layers", *Smart Mater. Struct.*, **13**, 1245-1257.
Pradhan, S.C., Loy, C.T., Lam, K.Y. and Reddy, J.N. (2000), "Vibration characteristics of functionally graded cylindrical shells under various boundary conditions", *Appl. Acoust.*, **61**(1), 119-129.
Put, S., Vleugels, J. and Van Der Biest, O. (2003), "Micro structural engineering of functionally graded materials

by electrophoretic deposition", *J. Mater. Process. Technol.,* **143**, 572-577.
Ramirez, F., Heyliger, P.R. and Pan, E. (2006), "Static analysis of functionally graded elastic anisotropic plates using a discrete layer approach", *Composites: Part B Eng*., **37**, 10-20.
Reddy, J.N. and Cheng, Z.Q. (2001), "Three-dimensional solutions of smart functionally graded plates", *J. Appl. Mech.,* **68**, 234-241.
Reddy, J.N. and Chin, C.D. (1998), "Thermo-mechanical analysis of functionally graded cylinders and plates", *J. Thermal Stresses,* **21**, 593-602.
Sachenkov, A.V. and Baktieva, L.U. (1978), "Approach to the solution of dynamic stability problems of thin shells (in Russian)", *Research on the Theory of Plates and Shells, Kazan State Univ*., **13**, 137-52.
Shahsiah, R. and Eslami, M.R. (2003), "Thermal buckling of functionally graded cylindrical shell", *J. Thermal Stresses,* **26**, 277-294.
Sheinman, I., Shaw, D. and Simitses, G.J. (1983), "Nonlinear analysis of axially loaded laminated cylindrical shells", *Comput. Struct.,* **16**(1-4), 131-137.
Shen, H.S. (2002), "Post-buckling of shears deformable laminated cylindrical shell", *Eng. Mech.,* **3**, 296-306.
Shen, H.S. (2003), "Post-buckling analysis of pressure loaded functionally graded cylindrical shells in thermal environments", *Eng. Struct*., **25**, 487-497.
Shen, H.S. and Noda, N. (2005), "Post-buckling of FGM cylindrical shell under combined axial and radial mechanical loads in thermal environments", *Int. J. Solids Struct.,* **42**, 4641-4662.
Shen, Z.J. and Nygren, M. (2002), "Laminated and functionally graded materials prepared by spark plasma sintering", *Key. Eng. Mater.,* **206**(2), 2155-2158.
Simitses, G.J. and Anastasiadis, J.S. (1991), "Buckling of axially loaded, moderately-thick, cylindrical laminated shells", *Compos. Eng.,* **1**(6), 375-391.
Sofiyev, A.H. (2003), "Dynamic buckling of functionally graded cylindrical shells under non-periodic impulsive loading", *Acta Mech.,* **165**, 153-162.
Sofiyev, A.H. (2004), "The stability of functionally graded truncated conical shells subjected to A-periodic impulsive loading", *Int. J. Solids Struct*., **41**(13), 3411-3424.
Sofiyev, A.H., Deniz, A., Akçay, I.H. and Yusufoglu, E. (2006), "The vibration and stability of a three-layered conical shell containing a FGM layer subjected to axial compressive load", *Acta Mech*. (in press).
Tabiei, A. and Simitses, G.J. (1994), "Buckling of moderately thick laminated cylindrical shells under trsion". *AIAA J.,* **21**, 639-647.
Tan, D. (2000), "Torsional buckling analysis of thin and thick shells of revolution", *Int. J. Solids Struct.,* **37**, 3055-3078.
Touloukian, Y.S. (1967), *Thermo-Physical Properties of High Temperature Solid Materials*, New York: Macmillan.
Vinson, J.R. and Sierakowski, R.L. (1986), *The Behavior of Structures Composed of Composite Material*. Nijhoft, Dordrecht.
Vodenitcharova, T. and Ansourian, P. (1996), "Buckling of circular cylindrical shells subjected to uniform lateral pressure", *Eng. Struct.,* **18**, 604-614.
Volmir, A.S. (1967), *Stability of Elastic Systems,* Nauka: Moscow. English Translation: Foreign Tech. Division, Air Force Systems Command. Wright-Patterson Air Force Base, Ohio, AD628508.
Warburton, G.B. (1965), "Vibration of thin cylindrical shells", *J. Mech. Eng. Sci.,* **7**, 399-407.
Weingarten, V.I. (1964), "Free vibrations of multilayered cylindrical shells", *Exp. Mech.,* 200-205.
Woo, J. and Mequid, S.A. (2001), "Nonlinear analysis of functionally graded plates and shallow shells", *Int. J. Solids Struct*., **38**, 7409-7421.
Xue, J. and Hoo Fatt, M.S. (2002), "Buckling of a non-uniform, long cylindrical shell subjected to external hydrostatic pressure", *Eng. Struct.,* **24**, 1027-1034.
Yang, J. and Shen, H.S. (2003), "Free vibration and parametric resonance of shear deformable functionally graded cylindrical panels", *J. Sound. Vib.,* **261**, 871-893.
Yang, J., Liew, K.M., Wu, Y.F. and Kitipornchai, S. (2006), "Thermo-mechanical post-buckling of FGM cylindrical panels with temperature-dependent properties", *Int. J. Solids Struct.,* **43**, 307-324.

Notation

$2a$	: Thickness of the FG layer
$E(z)$	: Young's modulus of the Ceramic-FGM-Metal shell
$\hat{E}$	: Young's modulus of the FG layer
E_{0c}, E_{0m}	: Young's moduli of purely ceramics and metal layers
E_c, E_m	: Young's moduli of the ceramics and metal surfaces of the FG layer
$\hat{E}/E_m$	: Dimensionless Young's modulus of the FG layer
e_x, e_y, e_{xy}	: Strain components on the reference surface of the cylindrical shell
h	: Total thickness of the cylindrical shell
L	: Length of the cylindrical shell
$L_{ij}(i,j = 1, 2)$	: Differential operators
M_x, M_y, M_{xy}	: Moment resultants
N	: Volume fraction index
N_x, N_y, N_{xy}	: Force resultants
N_x^0, N_y^0, N_{xy}^0	: Membrane forces prior to buckling
n, m	: Wave numbers
P, P_j $(j = -1 \div 3)$	: Material properties
Q_{ij}	: Reduced stiffness
P_{cr}	: Critical external pressure
R	: Radius of the cylindrical shell
T	: Temperature in Kelvin
T_{cr}	: Critical axial load
S_{cr}	: Critical torsional load
V_c, V_m	: Volume fractions of ceramics and metal surfaces, respectively
w	: Displacement of the middle surface in the inwards normal direction z
x, y, z	: Space coordinates
$\bar{z} = z/h$	: Dimensionless thickness coordinate
σ_x, σ_y, σ_{xy}	: Stress components
$\hat{\nu}$	: Poisson's ratios of the FG layer
ν_c, ν_m	: Poisson's ratios of the ceramics and metal surfaces of the FG layer
ν_{0c}, ν_{0m}	: Poisson's ratios of purely ceramic and metal layers
$\nu(z)$	: Poisson's ratio of the Ceramic-FGM-Metal shell
$\rho(z)$	: Density of the Ceramic-FGM-Metal shell
$\hat{\rho}$	: Density of the FG layer
ρ_c,ρ_m	: Densities of ceramic and surfaces of the FG layer
ρ_{0c}, ρ_{0m}	: Densities of purely ceramic and metal layers
ψ	: Stress function
$\xi(t)$, $\zeta(t)$	: Time dependent amplitudes